# Temperature dependence of the dc conductivity of undoped $a$-$Si_{1-x}Ge_x$:H alloys: Influence of metastability

R. Meaudre, M. Meaudre, and J. Chanel
*Département de Physique des Matériaux, Université de Lyon I, 43 boulevard du 11 Novembre 1918, 69622 Villeurbanne CEDEX, France*

(Received 26 November 1990)

The effects of alloying on the shape of the Arrhenius plots of the dc conductivity of glow-discharge $a$-$Si_{1-x}Ge_x$:H with $0 \le x \le 1$ have been investigated in the temperature range 30–250 °C. For $0 \le x \le 0.3$ the Arrhenius plots show a downward kink or negative concavity around a temperature $T_k$, whereas an upward kink or positive concavity is observed for $0.3 < x < 1$. Thermal quenching from 250 °C induces a lowering of a nonequilibrium dark dc conductivity in the first case and an increase in the second. Good correlation is found between $T_k$ and the equilibrium temperature $T_E$ (in the range 90 °C–190 °C) and suggests that the shape of the Arrhenius plots is essentially due to metastability. The possible implications to the change in the density-of-states distribution induced by Ge incorporation and by thermal quenching are discussed.

## I. INTRODUCTION

Amorphous hydrogenated silicon-germanium ($a$-$Si_{1-x}Ge_x$:H) alloys are potentially valuable materials for solar cells[1] and other device applications.[2,3] Their attraction comes from the possibility of adjusting their band gap continuously from 1.7 eV ($a$-Si:H) to about 1 eV ($a$-Ge:H). However, optoelectronic properties of $a$-$Si_{1-x}Ge_x$:H films are inferior to those of $a$-Si:H films[4] and the detailed distribution of the density of states (DOS) in the gap is still controversial.[5] In recent papers[6,7] we have shown that the study of Arrhenius plots of the dc conductivity of undoped $a$-Si:H can shed some light on the change of DOS in relation to metastability. Since thermally induced metastable phenomena have recently been observed[8–10] in $a$-$Si_{1-x}Ge_x$:H we here propose to extend this research on the connection which may exist between the shape of the dc conductivity versus $T^{-1}$ characteristics and the dependence of the DOS with temperature.

## II. EXPERIMENTAL

The samples have been deposited in the ARCAM reactor[11] by using the conventional diode radio-frequency (13.6 MHz) decomposition of $SiH_4$–$GeH_4$–$H_2$ mixtures. The dilution ratio $R_D = [GeH_4]/([GeH_4]+[H_2])$ is set to 0.10 for $a$-SiGe:H films and to 0.01 for $a$-Ge:H films. The solid-phase Ge content is changed by varying the ratio $R_G = [GeH_4]/([GeH_4]+[SiH_4])$. Preparation conditions and characteristics of the films are given in Table I. Details about film analysis, optical properties, and conductivity measurements are given elsewhere.[6,12–16] We only recall here that conductivity was studied in coplanar configuration, the samples were first annealed at 250 °C (the substrate temperature during deposition) for 30 min and then cooled to room temperature at quench or slow cool rates, and the conductivity-temperature characteristics were recorded as the samples were warmed up to 250 °C (heating rate 1 °C/min). It is worth noting that the curves obtained after slow cool can also be obtained by slowly cooling from 250 °C.

## III. RESULTS

Though unimportant in the context of this paper, we note in passing that the Tauc gap $E_G$ of our $a$-SiGe:H alloys varies linearly with the atomic fraction $x$ of Ge ac-

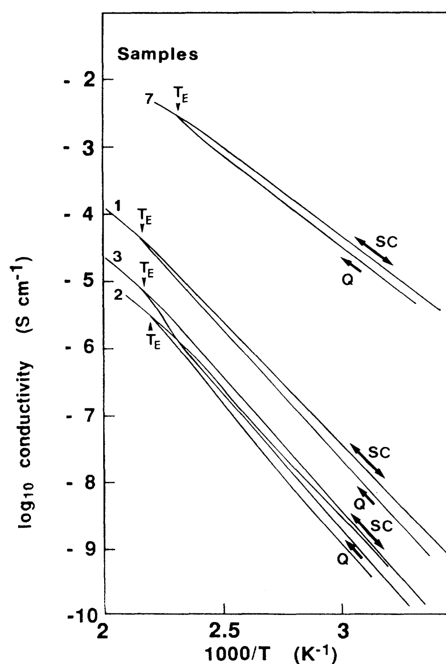


FIG. 1. Temperature dependence of the dc conductivity of samples showing a downward kink and $\sigma_Q < \sigma_{SC}$. Cooling rates from 250 °C to room temperature: $Q$, 10 °C/s; SC, 0.05 °C/s.

 ©1991 The American Physical Society

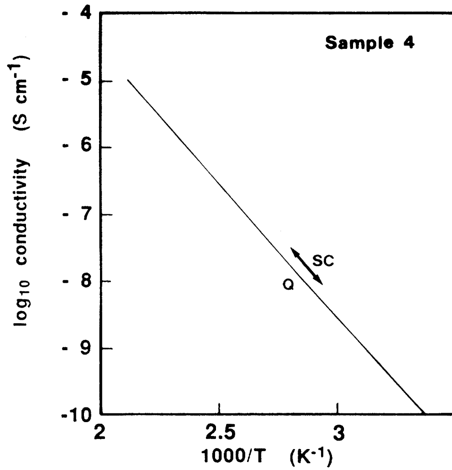


FIG. 2. Temperature dependence of the dc conductivity of sample 4 showing neither quenching effect nor kink. Cooling rates from 250 °C to room temperature: $Q$, 10 °C/s; SC, 0.05 °C/s.

cording to the equation $E_G$ (eV)$=1.74-0.77x$ in excellent agreement with the results of Mackenzie *et al.*[17]

Figures 1, 2, and 3 show typical Arrhenius plots of the conductivity of our undoped films. The following are observed.

(i) $0 \le x < 0.3$; $E_G > 1.5$ eV, there is a downward kink, and the conductivity $\sigma_Q$ measured after quenching is lower than the conductivity $\sigma_{SC}$ measured after slow cooling for temperature lower than $T_E$. $T_E$ is the temperature above which the dc conductivity is independent of the prior thermal history.

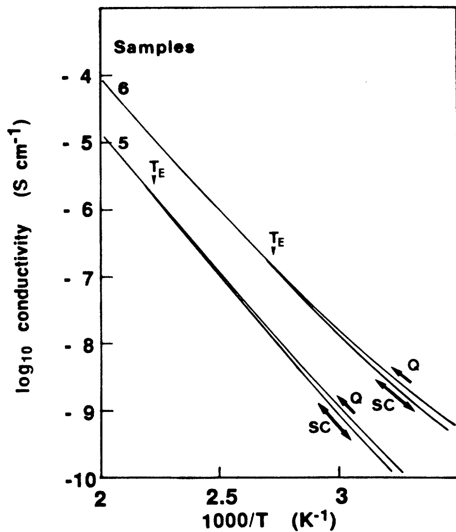


FIG. 3. Temperature dependence of the dc conductivity of Ge-rich samples ($x > 0.3$) showing an upward curvature and $\sigma_Q > \sigma_{SC}$. Cooling rates from 250 °C to room temperature: $Q$, 10 °C/s; SC, 0.05 °C/s.

TABLE I. Preparation conditions and characteristics of the samples. The Ge and H contents have been deduced from Rutherford backscattering of $\alpha$ particles and elastic recoil detection analysis, respectively (Ref. 13). The optical gap $E_g$ has been derived using classical Tauc's plot, the Urbach energy $E_u$ from photothermal deflection spectroscopy data (Ref. 5) and the density of states at the Fermi level $N(E_F)$ from space-charge-limited current measurements (Ref. 14). $E_a$ is the dark conductivity activation energy measured around 250 °C [high temperature (HT)] and 30 °C after slow cool [low temperature (LT)]. $\sigma_0^*$ is the measured preexponential factor of the conductivity, $T_E$ and $T_k$ the equilibration and kink temperatures, respectively.

| Samples | Substrate $T$ (°C) | Power (mW/cm$^2$) | $d$ ($\mu$m) | [Ge]/([Si]+[Ge]) | [H]/([Si]+[Ge]) | $E_g$ (eV) | $E_u$ (meV) | $N(E_F)$ (cm$^{-3}$eV$^{-1}$) | $E_a$ (eV) HT | $E_a$ (eV) LT | $\sigma_0^*$ (S cm$^{-1}$) HT | $\sigma_0^*$ (S cm$^{-1}$) LT | $T_E$ (°C) | $T_k$ (°C) |
|---|---|---|---|---|---|---|---|---|---|---|---|---|---|---|
| 1 | 200 | 20 | 1.7 | 0 | 0.13 | 1.7 | 51 | $5\times10^{15}$ | 0.55 | 0.74 | 35 | $4\times10^{3}$ | 190 | 180 |
| 2 | 250 | 10 | 1.3 | 0.19 | 0.11 | 1.6 | 56 | $7\times10^{16}$ | 0.59 | 0.75 | 9 | 500 | 180 | 170 |
| 3 | 250 | 10 | 1.45 | 0.25 | 0.1 | 1.55 | 56 | $7\times10^{16}$ | 0.61 | 0.77 | 35 | $1.5\times10^{3}$ | 190 | 180 |
| 4 | 250 | 10 | 1.12 | 0.3 | 0.1 | 1.5 | 58 | $1.5\times10^{17}$ | 0.78 | 0.78 | $1.6\times10^{3}$ | | | |
| 5 | 250 | 10 | 1.1 | 0.36 | 0.09 | 1.46 | 60 | $4\times10^{17}$ | 0.9 | 0.76 | $1.5\times10^{4}$ | 250 | 175 | 145 |
| 6 | 250 | 10 | 1.45 | 0.6 | 0.08 | 1.3 | 69 | $\ge10^{18}$ | 0.83 | 0.65 | $2.6\times10^{4}$ | 110 | 90 | 85 |
| 7 | 250 | 100 | 1.7 | 1 | 0.065 | 1.03 | 49 | $\ge10^{18}$ | 0.35 | 0.52 | 36 | $3.9\times10^{3}$ | 160 | 150 |

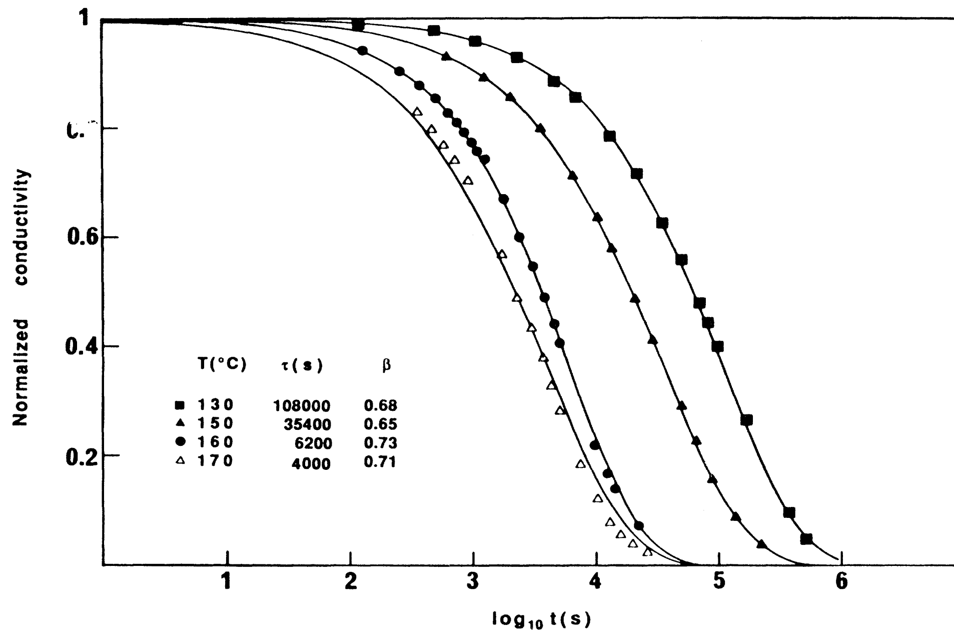


FIG. 4. Example of time dependence of the normalized reduced conductivity of sample 2 at different temperatures. The solid lines are fitted to the data using the function $\exp[-(t/\tau)^{\beta}]$ with $\beta$ and $\tau$ values given in the figure. The activation energy of $\tau$ is $\sim 1.4$ eV.

(ii) $x \sim 0.3$; $E_G \sim 1.5$ eV, the Arrhenius plot is a straight line. No influence of cooling rates can be observed.

(iii) $0.3 < x \leq 0.6$; $E_G < 1.5$ eV, there is an upward kink, and $\sigma_Q > \sigma_{SC}$.

(iv) For $x=1$, $E_G = 1.03$ eV, corresponding to pure *a*-Ge:H we find again behavior (i).

The changes in conductivity induced by quenching are reversible and we have been able to cycle between quenched and slow-cooled states repeatedly. After quenching and stabilizing the film substrate at $T < T_E$, the conductivity $\sigma(t)$ increases ($0 \leq x < 0.3$ or $x=1$) or decreases ($0.3 < x \leq 0.6$) monotonically to an equilibrium value. Figure 4 shows an example of the time dependence of the normalized conductivity. The evolution is not a simple exponential; increasing the temperature speeds the relaxation process. For every type of film, and as already extensively shown for pure *a*-Si:H (Ref. 12) and *a*-GeH,[18] the behavior of $\sigma(t)$ is well described by a stretched exponential function $\exp[-(t/\tau)^{\beta}]$. The time constant $\tau$ is thermally activated.

## IV. DISCUSSION

### A. Comparison with other results

As already observed[6,7] in the case of undoped or doped *a*-Si:H it is interesting to note that there is a perfect correlation between the kink curvature and the conductivity change after a quench. More precisely we see that when there is an upward (downward) kink, the quenched conductivity is higher (lower) than that obtained after slow cooling. To our knowledge such a change in the shapes of the characteristics and in quenching behavior has never been pointed out by the many researchers who have studied the electronic properties of *a*-SiGe alloys.[4,8–10,17,19,20] However, it should be noted that Bullot *et al.*[19] have only studied Si-rich *a*-SiGe:H alloys ($x \leq 0.38$) and limited their conductivity study in the range 20 °C–100 °C, whereas for our Si-rich *a*-SiGe:H alloys we observed kinks at temperatures of about 180 °C–190 °C (Fig. 1, Table I). Aljishi, Smith, and Wagner[4] in their study of *a*-SiGe:H,F alloys have also limited their temperature range up to 60 °C. On the contrary, Mackenzie *et al.*[17,20] studied the dark conductivity of *a*-SiGe:H and *a*-SiGe:H,F up to 230 °C. They claimed that practically all their alloys show a downward kink up to $x \sim 0.53$. However, they pointed out that a sample with $x=0.5$ does not show a kink.[17] It should be noticed that their *a*-SiGe:H was grown from a $SiH_4$-$GeH_4$ mixture, whereas we used a mixture diluted in hydrogen. Another interesting observation of Bullot *et al.*[19] is that samples with $x=0.38$ ($E_G \approx 1.5-1.6$ eV) show no reversible change in the dark and photoconductive properties as upon light soaking. This transition around $E_G \approx 1.4$ eV of the susceptibility to light soaking and of other properties of *a*-SiGe alloys have also been reported by Wagner *et al.*[21] and Stutzmann *et al.*[22] It is roughly in this range of $x$ values that we observed no quenching effects.

In their study of $a$-$Si_{1-x}Ge_x$:H,F films with an optical gap down to 1.33 eV, corresponding to $x \sim 0.5$, Liu *et al.*[8,9] and Shimizu *et al.*[10] observed that $\sigma_Q < \sigma_{SC}$ for $T_E \leq 125$ °C–140 °C and in agreement with our above observation, $\sigma_Q < \sigma_{SC}$ corresponds to a downward kink in the Arrhenius plot of the conductivity.

### B. Explanation of the kink

Before discussing the shape of the Arrhenius plots we wished first to exclude an explanation of the upward kinks observed for $0.3 < x \leq 0.6$ in terms of change of the conduction path. Indeed, it is well known that conduction in amorphous materials is dependent on the defect-state distribution. The presence of both band-tail states, near the mobility edges, and a high density of localized states deep in the gap, can lead to several transport channels that dominate conduction in different temperature regimes.[23] At high temperatures, conduction is due to carriers excited into extended states. As the temperature is lowered the conduction path shifts to lower energies, below a mobility edge; this leads to an upward curvature in the Arrhenius plot of the conductivity. If the curvatures observed in Fig. 3 were due to the emergence of hopping conduction near the mobility edge $E_C$ or at the Fermi level as the temperature is lowered, one would have to admit that the hopping process begins to play a role when the conductivity is near $5\times10^{-7}$ S cm$^{-1}$ ($T_K=145$ °C) for sample 5 and near $5\times10^{-8}$ S cm$^{-1}$ ($T_k=85$ °C) for sample 6 in disagreement with an increase of the DOS below $E_C$ or near $E_F$ with Ge content[16] (Table I). A transition from extended states to localized states conduction has been observed below room temperature by Aljishi, Smith, and Wagner[4] in *a*-SiGe:H, F alloys. The magnitude of the dc conductivity and activation energy we measured near or just above room temperature in our samples (Table I) agree quite well with their results. Following these authors and also Bullot *et al.*[19] we then assume that in the temperature range considered here, conduction arises from electrons excited above a mobility edge $E_C$. This assumption immediately leads to the conductivity

$$\sigma(T)=\sigma_0 \exp-[(E_C-E_F)/kT] , \tag{1}$$

where $E_F$ is the Fermi level and $\sigma_0$ the preexponential factor of the conductivity which is temperature independent and has a value of about 50–150 S cm$^{-1}$.[24,25] Then according to Eq. (1), a kink is related to the temperature dependence of $E_C-E_F$. More precisely, we can say that a kink necessarily arises from a sharp change in the temperature dependence of $E_C-E_F$. $E_C-E_F$ is temperature dependent because the gap $E_G$, the neutrality equation, and the DOS depend on the temperature. Though we do not have much information about the change of the gap with temperature in *a*-SiGe:H, we exclude, as is the case for *a*-Si:H, that this could explain the kink. Indeed it would be very surprising that the shrinking gap leads to a downward kink for $x<0.3$ and an upward kink for $x>0.3$. Let us now examine the two other possibilities.

The Fermi level is determined by solving the neutrality equation

$$n+D^-=p+D^+ , \tag{2}$$

where $n$ and $p$ are the electron and hole densities in extended and localized band-tail states, and $D^-$ and $D^+$ are the densities of charged defects, such as dangling bonds. Equation (2) can be written as

$$\int g_c(E,T)f(E,E_F,T)dE+\int g_D(E,T)f^-(E,E_F,T)dE =\int g_v(E,T)[1-f(E,E_F,T)]dE +\int g_D(E,T)f^+(E,E_F,T)dE , \tag{3}$$

where $g_c$, $g_v$, and $g_D$ are the DOS for the conduction, the valence, and the defect bands, respectively, $f$ is the Fermi function, and $f^-$ and $f^+$ are the distribution functions for correlated states as given by Okamoto *et al.*[26]

Then according to Eq. (3), the Fermi level can be temperature dependent because (i) $f, f^-, f^+$ are temperature dependent: that is what is called the statistical shift;[24] (ii) $g_c$, $g_v$, and $g_D$ can be temperature dependent if thermal-equilibrium processes are present in the sample.[6,27] Therefore, a kink will appear if there is a (sudden) change in the magnitude of the statistical shift of $E_F$ or a change in the temperature dependence of the DOS. In previous papers[7,28] about *a*-Si:H we have investigated both possibilities, the conclusion being that although a contribution to the kink from the statistical shift cannot be totally excluded, the observed facts suggest thermal equilibrium processes as a more natural and preferable explanation. Since it is shown in Figs. 1–3 that both kink and metastability are observed in our samples and that $T_E$ and $T_k$ (the kink temperature at which the produced high- and low-temperature lines cross in the Arrhenius plot) are correlated (Table I), we propose that the kink is caused by the freezing of the sample in a nonequilibrium configuration, and that the kink is essentially due to a sudden change in the temperature dependence of the DOS. At high temperature, $T>T_E$, the sample is allowed to equilibrate and then two factors contribute to the shape of the conductivity plot: the statistical shift and the temperature dependence of the DOS. For low temperature, $T<T_E$ the statistical shift is always present but the DOS is frozen because the time needed to reach equilibrium is much longer than the experimental time scale. Then there is a sudden change in the temperature dependence of the DOS at $T\approx T_E\approx T_k$ at which the kink happens. Let us now examine the shape of the conductivity plot.

A linear Arrhenius plot for $\sigma(T)$ means, according to Eq. (1), a linear $E_C-E_F$ temperature dependence

$$(E_C-E_F)_T=(E_C-E_F)_0-\gamma kT , \tag{4}$$

which with Eq. (1) immediately leads to

$$\sigma(T)=\sigma_0^* \exp(-E_a/kT) , \tag{5}$$

where $E_a=(E_C-E_F)_0$ is the temperature-independent activation energy and corresponds to $E_C-E_F$ extrapolated to $T=0$ K (Fig. 5) and $\sigma_0^*=\sigma_0\exp(\gamma)$ is the measured preexponential factor. $\gamma$ includes the red shift of the gap ($\gamma_G$) and the shift of $E_F$ ($\gamma_F$),

$$\gamma=\gamma_G/2+\gamma_F$$

($\gamma_G/2$ is taken when one assumes a uniform scaling of the gap energies and $E_F$ around midgap).

In order to explain the three typical behaviors of the Arrhenius plots shown in Figs. 1–3, the Fermi level must behave (excluding $\gamma_G$ for clarity) as shown in Fig. 5. A downward (upward) kink means that $E_F$ in the high-temperature range is further (closer) to the mobility edge $E_C$ than it would be without a kink. Everything happens as if, after a quench, the sample partially "remembered" this position of $E_F$ and had a lower (higher) conductivity. This is easy to understand in terms of the glass model,[29] and seems an argument in favor of the explanation of the kink by this model: if the kink resulted only from a statistical shift there would be no reason for the samples to "remember" the position of $E_F$ at higher temperature.

The nearly constant values of $E_C - E_F$ schematically shown in Figs. 5(a) and 5(c) at low temperatures and in the whole temperature range in cases (b) simply mean that taking the experimental values of $\sigma_0^*$ (Table I), $\sigma_0 \approx 50-150$ S cm$^{-1}$, and $\gamma_G = 5$, it is easily shown that $|\gamma_F|$ has lower values (of order 1.5–2) in the low-temperature range than in the high-temperature range where $\gamma_F \sim 3-4$. These low values of $|\gamma_F|$ confirm earlier calculations and experiments[7,25] which show that, at low temperatures, the statistical shift of $E_F$ is weak. They also confirm that, as the temperature rises, the shift of $E_F$ becomes important when the DOS begins to change above $T_E$.

### C. The change in the DOS distribution induced by quenching and by the variation of temperature

In the following we discuss the expected changes in the DOS which would explain the previous experimental results and as in Sec. III we distinguish different composition ranges of the alloys.

(i) $0 \leq x < 0.3$. In this comparison range the alloys behave essentially as pure *a*-Si:H, therefore, as suggested by Wagner *et al.*[30] and Chahed *et al.*,[5] we suppose that the $D^{0+}$(Si)/$D^{0-}$(Si) levels associated with Si dominate. We then adopt the same interpretation as that already given in the case of *a*-Si:H.[6] Besides an increase of the defect density with temperature, the temperature dependence of the energy $E^{0-}(T)$ of the peak of the $D^{0-}$(Si) levels is given by

$$E^{0-}(T) - E_v = E_{A0} + E_W^2/kT . \quad (6)$$

$E_v$ is the valence-band mobility edge and $E_{A0}$ and $E_W$ are the energy of the maximum and the width of the distribution of annealing energies of dangling bonds as given by Smith *et al.*[31]

$E_F$ is roughly pinned at $E^{0-} - U/2$, $U$ being the positive correlation energy of about 0.2 eV.[22] Quenching from $T_Q > T_E$ freezes the $D^{0-}$ and $D^{0+}$ peaks at their equilibrium location at $T_Q$ provided that equilibrium was achieved. Slow cooling freezes the peaks near $T_E$ and then according to Eq. (6): $E_{F(SC)} = E^{0-}(T_E) - U/2 > E^{0-}(T_Q) - U/2 = E_{F(Q)}$, showing that $\sigma_{SC} > \sigma_Q$. Below $T_E$, the $D^{0-}$ and $D^{0+}$ peaks are frozen, $E_F$ is temperature independent. When $T$ increases above $T_E$, $E^{0-}(T)$ and $E_F(T)$ decrease [Eq. (6)]. These two results qualitatively explain the curves in Figs. 1 and 5(a).

(ii) $0.3 < x \leq 0.6$. In that range of Ge-rich alloys the Ge dangling bonds dominate[5,22,30] and we then adopt for the DOS the model given by Stutzmann *et al.*[22] and that is shown in Fig. 6. Considering the different bonding energies between Si and Ge atoms and the possibility that the microscopic strain is preferentially concentrated on the softest bonds, i.e., Ge—Ge, these authors proposed that the deepest valence band-tail states are preferentially caused by localized bonding orbitals of weak Ge—Ge bonds, whereas Si—Ge and Si—Si bonds lead to more

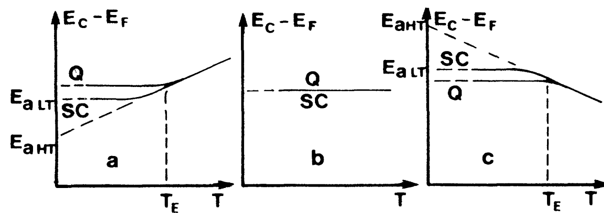


FIG. 5. Schematic representation of the behavior of the Fermi level with temperature, after slow cool (SC) and quenching ($Q$). $E_C$ is the conduction-band mobility edge. $E_{a\mathrm{HT}}$ and $E_{a\mathrm{LT}}$ are the activation energies of dark conductivity in the high- and low-temperature ranges separating the kink, respectively. For simplicity the gap shrinking has been neglected and the constant values of $E_C - E_F$ simply mean that in the considered temperature range $|\gamma_F|$ is smaller than in the other part of the curve. Curves $a,b,c$, explain the Arrhenius plots shown in Figs. 1, 2, and 3, respectively.

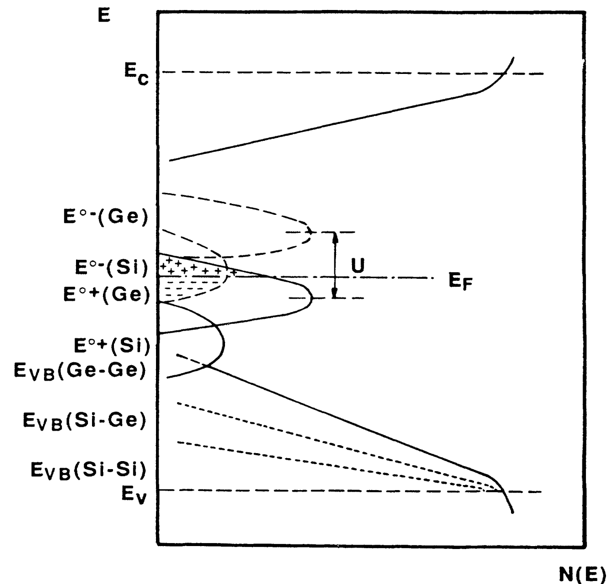


FIG. 6. Schematic model of the DOS in Ge-rich ($x > 0.3$) *a*-$Si_{1-x}Ge_x$:H alloys according to Stutzmann *et al.* (Ref. 22). VB is the valence-band tail; the energies $E^{0+}$ and $E^{0-}$ correspond to singly and doubly occupied dangling bonds; $E_F$ denotes the position of the Fermi level, $U$ is the correlation energy of dangling bonds.

shallow states. This picture is schematically shown in Fig. 6. The position of the Fermi level is imposed by the neutrality condition which reads $D^-(\text{Si})=D^+(\text{Ge})$; these charges are presented in Fig. 6 Considering now the different energy levels, it is seen that the energy $E^{0+}(\text{Ge})-E_{\text{VB}}(\text{Ge—Ge})$ needed to create a $D^0(\text{Ge})$ can be lower than the energy $E^{0+}(\text{Si})-E_{\text{VB}}(\text{Si—Si})$ needed to create a $D^0(\text{Si})$ [the energy gained to transform them eventually into $D^+(\text{Ge})$ and $D^-(\text{Si})$ being comparable]. As the temperature rises above $T_E$, the density of $D^{0+}(\text{Ge})$ levels increases more than the density of $D^{0+}(\text{Si})$, so does $D^+(\text{Ge})$ as compared to $D^-(\text{Si})$. In order to maintain the charge neutrality, it is easily shown from Fig. 6 that $E_F$ must increase. This qualitatively explains the kink and quenching effects in Fig. 3 and the decrease in $E_C-E_F$ shown in Fig. 5(c). It is worth noting that this picture could also explain the increase of the dark conductivity and the decrease of the photoconductivity upon light soaking observed in these Ge rich films.[32]

From measurements of gap states by modulated photocurrent spectroscopy, Tsutsumi *et al.*[33] also proposed that a switch of the predominant deep centers occurs from Si dangling bonds to Ge dangling bonds as the Ge concentration approaches 35 at. %, which corresponds to an optical gap of around 1.5 eV. However, contrary to Stutzmann *et al.*[22] it is suggested that the $D^{0-}(\text{Ge})$ center is located deeper by about 0.1 eV than the $D^{0-}(\text{Si})$ center. Using the preceding reasoning it is easily shown that such a DOS cannot explain our results. Furthermore, the energy location of the $D^{0-}(\text{Ge})$ at 0.3–0.4 eV below $E_C$, as proposed by Tsutsumi *et al.*,[33] and a correlation energy of about 0.2 eV lead to $E_C-E_F\sim0.4$–$0.5$ eV, hardly compatible with our measured activation energy. We then preferred the model given by Stutzmann *et al.*[22]

(iii) $x\sim0.3$. The densities of Si- and Ge-like dangling bonds should then be comparable. It is easily understood that in this Si-rich alloy the fact that weak Ge—Ge bonds are easier to break than weak Si—Si bonds can be compensated by the higher density of weak Si—Si bonds relative to weak Ge—Ge bonds, so that $D^-(\text{Si})$ and $D^+(\text{Ge})$ increase in the same way as temperature rises above $T_E$, maintaining charge neutrality without any change in $E_F$. Arrhenius plots of conductivity are then straight lines and no quenching effects can be observed.

(iv) $x=1$. In pure *a*-Ge:H the dominant deep defect-state distribution is solely due to Ge dangling bonds.[15] Therefore we can expect that the explanation given in (i) prevails for *a*-Ge:H and *a*-Si:H, explaining well why these two types of films have quite similar behaviors (Fig. 1).

## V. CONCLUSION

The Arrhenius plots of dc conductivity of *a*-SiGe:H alloys studied in the range 30 °C–250 °C show three typical behaviors. For pure *a*-Si:H, pure *a*-Ge:H, and Si-rich *a*-$\text{Si}_{1-x}\text{Ge}_x$:H ($x<0.3$), a downward kink is accompanied with a quenched conductivity lower than the conductivity obtained after a slow cool. The kink is essentially due to metastability and occurs near an equilibrium temperature $T_E$ where the DOS, dominated by Si dangling bonds, or Ge dangling bonds in the case of pure *a*-Ge:H, is allowed to equilibrate and shifts towards $E_v$ as the temperature rises. $T_E$ is in the 160 °C–200 °C range. For Ge-rich alloys ($0.3<x\le0.6$) an upward kink coupled with an increased quenched conductivity is observed. The defect states due to Ge dangling bonds dominate and are more susceptible to temperature than the Si-like defects. However, both kinds of defects coexist in the same energy region near midgap and the maintain of charge neutrality imposes an increase of the Fermi level when the temperature rises, thus explaining the kink curvature and the higher quenched conductivity. An equilibrium temperature $T_E$ of order 90 °C is observed for $x=0.6$. In the intermediate composition range, $x\approx0.3$, Si- and Ge-like DOS should increase with temperature in a similar way because, though the weak Ge—Ge bonds are easier to break, they are fewer than the weak Si—Si bonds. The neutrality can be satisfied without a shift of $E_F$. Straight Arrhenius plots and no quenching effects are then observed.

Finally this work adds to the mounting evidence that in undoped or doped *a*-Si:H, *a*-Ge:H, *a*-SiGe:H, and *a*-SiC:H (Ref. 34) alloys, there is a perfect correlation between the kink curvature and the conductivity change after a quench. It is interesting to note that it has recently been found that $T_E\ge230$ °C for undoped *a*-SiN:H films with $E_G\ge1.8$ eV.[35] This is in agreement with our observation of no kink up to 200 °C in that kind of film.[36] The kinks currently observed in the Arrhenius plots of the conductivity should then mainly be due to metastability.

## ACKNOWLEDGMENTS

We are grateful to C. Godet and D. Conne for providing the samples. This work was partially supported by Agence Française pour la Maîtrise de l'Energie, Programme Interdisciplinaire de Recherche sur les Sciences pour l'Energie et les Matières Premières (AFME-PIRSEM-CNRS contracts) and Commission of the European Communities (CEC contracts). The Département de Physique des Matériaux is "Unité associée au Centre National de la Recherche Scientifique No. 172."

[1]C. M. Fortmann, S. S. Hegedus, and W. A. Buchanan, J. Non-Cryst. Solids **115**, 21 (1989).

[2]P. D. Deimel, B. Heimhofer, G. Krötz, G. Müller, and J. Wind, J. Non-Cryst. Solids **115**, 186 (1989).

[3]D. S. Shen, J. P. Conde, V. Chu, S. Aljishi, and W. Wagner, in *Amorphous Silicon Technology,* edited by A. Madan, M. J. Thomson, P. C. Taylor, P. G. Le Comber, and Y. Hamakawa, MRS Symposia Proceedings No. 118 (Materials Research Society, Pittsburgh, 1988), p. 457.

[4]S. Aljishi, Z. E. Smith, and S. Wagner, in *Advances in Amorphous Semiconductors,* edited by H. Fritzsche (World Scientific, Singapore, 1989), p. 887.

[5] L. Chahed, A. Gheorghiu, M. L. Theye, I. Ardelean, C. Senemaud, and C. Godet, J. Non-Cryst. Solids **114**, 471 (1989).
[6] M. Meaudre, P. Jensen, and R. Meaudre, Philos. Mag. B (to be published).
[7] P. Jensen, R. Meaudre, and M. Meaudre, J. Phys. Condens. Matter **2**, 4785 (1990).
[8] J. Z. Liu, V. Chu, D. S. Shen, D. Slobodin, and W. Wagner, Phys. Rev. B **40**, 6424 (1989).
[9] J. Z. Liu, D. S. Shen, P. Roca i Cabarrocas, H. R. Park, and S. Wagner, in *Amorphous Silicon Technology,* MRS Symposia Proceedings No. 192 (Materials Research Society, Pittsburgh, 1990), p. 701.
[10] T. Shimizu, X. Xu, H. Sasaki, H. Yan, A. Morimoto, and M. Kumeda, in *Amorphous Silicon Technology,* MRS Symposia Proceedings No. 192 (Materials Research Society, Pittsburgh, 1990), p. 695.
[11] P. Roca i Cabarrocas, B. Equer, J. Huc, A. Lhoret, and J. P. M. Schmitt, in *Proceedings of the Seventh Photovoltaic Solar Energy Conference, Sevilla, 1986,* edited by A. Goetzberg, W. Palz, and G. Willeke (Reidel, Dordrecht, 1987), p. 533.
[12] R. Meaudre, P. Jensen, and M. Meaudre, Phys. Rev. B **38**, 12 449 (1988).
[13] C. Godet, A. Lhoret, and J. P. Stoquert, *9th European Communities Photovoltaic Solar Energy Conference, Freiburg, 1989,* edited by W. Palz, G. T. Wrixon, and P. Helm (Kluwer, Dordrecht, 1989), p. 70.
[14] A. Labdi, C. Godet, B. Equer, and G. de Rosny, J. Appl. Phys. (to be published).
[15] C. Godet, Y. Bouizem, L. Chahed, I. Elzawawi, M. L. Theye, M. Meaudre, R. Meaudre, S. Basrour, and J. C. Bruyere (unpublished).
[16] D. Mencaraglia, J. P. Kleider, C. Longeaud, Z. Djebbour, M. Hadrami, C. Godet, and R. Vanderhaghen, in *9th European Communities Photovoltaic Solar Energy Conference, Freiburg, 1989,* edited by W. Palz, G. T. Wrixon, and P. Helm (Kluwer, Dordrecht, 1989), p. 91.
[17] K. D. Mackenzie, J. R. Eggert, D. J. Leopold, Y. M. Li, S. Lin, and W. Paul, Phys. Rev. B **31**, 2198 (1985).
[18] M. Meaudre, R. Meaudre, and C. Godet, J. Phys. Condens. Matter (to be published).
[19] J. Bullot, M. Galin, M. Gauthier, and B. Bourdon, J. Phys. (Paris) **44**, 713 (1983).
[20] K. D. Mackenzie, J. H. Burnett, J. R. Eggert, Y. M. Li, and W. Paul, Phys. Rev. B **38**, 6120 (1988).
[21] S. Wagner, V. Chu, J. P. Conde, and I. Z. Liu, J. Non-Cryst. Solids **114**, 453 (1989).
[22] M. Stutzmann, R. A. Street, C. C. Tsai, J. B. Boyce, and S. E. Ready, J. Appl. Phys. **66**, 569 (1989).
[23] N. F. Mott and E. A. Davis, *Electronic Processes in Non-Crystalline Materials* (Clarendon, Oxford, 1979).
[24] J. Overhof and P. Thomas, *Electronic Transport in Hydrogenated Amorphous Silicon,* Springer Tracts in Modern Physics Vol. 114 (Springer, Berlin, 1989).
[25] R. Meaudre, P. Jensen, M. Meaudre, and C. Godet, J. Non-Cryst. Solids **114**, 360 (1989).
[26] H. Okamoto and Y. Hamakawa, Solid State Commun. **24**, 23 (1977).
[27] R. A. Street and K. Winer, Phys. Rev. B **40**, 6236 (1989).
[28] P. Jensen and R. Meaudre, J. Phys. Condens. Mater. **2**, 10 411 (1990).
[29] R. Zallen, *The Physics of Amorphous Solids* (Wiley, New York, 1983).
[30] S. Wagner, V. Chu, D. S. Chen, J. P. Conde, S. Aljishi, and Z. E. Smith, in *Amorphous Silicon Technology,* edited by A. Madan, M. J. Thomson, P. C. Taylor, P. G. Le Comber, and Y. Hamakawa, MRS Symposia Proceedings No. 118 (Materials Research Society, Pittsburgh, 1988), p. 623.
[31] Z. E. Smith, S. Aljishi, D. Slobodin, V. Chu, S. Wagner, P. M. Lenahan, R. R. Arya, and M. S. Bennet, Phys. Rev. Lett. **57**, 2450 (1986).
[32] V. Chu, J. P. Conde, D. S. Shen, S. Aljishi, and W. Wagner, in *Amorphous Silicon Technology,* edited by A. Madan, M. J. Thomson, P. C. Taylor, P. G. Le Comber, and Y. Hamakawa, MRS Symposia Proceedings No. 118 (Materials Research Society, Pittsburgh, 1988), p. 167.
[33] Y. Tsutsumi, H. Okamoto, and Y. Hamkawa, Philos. Mag. B **60**, 695 (1989).
[34] X. Xu, A. Okumura, A. Morimoto, M. Kumeda, and T. Shimizu, Phys. Rev. B **38**, 8371 (1988).
[35] X. Xu and T. Shimizu, Philos. Mag. Lett. **62**, 119 (1990).
[36] M. Meaudre and R. Meaudre, Philos. Mag. B **55**, 417 (1987).